Biomedical Optics EXPRESS

Numerical comparison of X-ray differential phase contrast and attenuation contrast

Dieter Hahn,[1,*] Pierre Thibault,[1] Martin Bech,[1] Marco Stockmar,[1] Simone Schleede,[1] Irene Zanette,[2] Alexander Rack,[2] Timm Weitkamp,[3] Aniko Sztrókay,[4] Thomas Schlossbauer,[4] Fabian Bamberg,[4] Maximilian Reiser,[4] and Franz Pfeiffer[1]

[1] *Technische Universität München - 85748 Garching, Germany*
[2] *European Synchrotron Radiation Facility - 38043 Grenoble, France*
[3] *Synchrotron Soleil - 91192 Gif-sur-Yvette, France*
[4] *Institute for Clinical Radiology, Ludwig Maximilians University - 81377 Munich, Germany*
[*] *dieter.hahn@ph.tum.de*

Abstract: We present a numerical tool to compare directly the contrast-to-noise-ratio (CNR) of the attenuation- and differential phase-contrast signals available from grating-based X-ray imaging for single radiographs. The attenuation projection is differentiated to bring it into a modality comparable to the differential phase projection using a Gaussian derivative filter. A Relative Contrast Gain (RCG) is then defined as the ratio of the CNR of image values in a region of interest (ROI) in the differential phase projection to the CNR of image values in the same ROI in the differential attenuation projection. We apply the method on experimental data of human breast tissue acquired using a grating interferometer to compare the two contrast modes for two regions of interest differing in the type of tissue. Our results indicate that the proposed method can be used as a local estimate of the spatial distribution of the ratio δ/β, i.e., real and imaginary part of the complex refractive index, across a sample.

OCIS codes: (110.7440) X-ray imaging; (100.2960) Image analysis; (100.2000) Digital image processing.

References and links

1. U. Bonse and M. Hart, "An x-ray interferometer with long separated interfering beam paths," Appl. Phys. Lett. **6**, 155–156 (1965).
2. R. Fitzgerald, "Phase-sensitive x-ray imaging," Phys. Today **53**, 23–26 (2000).
3. A. Momose, "Phase-sensitive imaging and phase tomography using x-ray interferometers," Opt. Express **11**, 2303–2314 (2003).
4. A. Momose, T. Takeda, A. Yoneyama, I. Koyama, and Y. Itai, "Phase-contrast x-ray imaging using an x-ray interferometer for biological imaging," Anal. Sci. 17(Suppl.), i527–i530 (2001).
5. A. Momose, S. Kawamoto, I. Koyama, Y. Hamaishi, K. Takai, and Y. Suzuki, "Demonstration of x-ray Talbot interferometry," Jpn. J. Appl. Phys. **42**, L866–L868 (2003).
6. F. Pfeiffer, T. Weitkamp, O. Bunk, and C. David, "Phase retrieval and differential phase-contrast imaging with low-brilliance x-ray sources," Nat. Phys. **2**, 258–261 (2006).
7. F. Pfeiffer, C. Kottler, O. Bunk, and C. David, "Hard x-ray phase tomography with low-brilliance sources," Phys. Rev. Lett. **98**, 105–108 (2007).
8. T. Weitkamp, A. Diaz, C. David, F. Pfeiffer, M. Stampanoni, P. Cloetens, and E. Ziegler, "X-ray phase imaging with a grating interferometer," Opt. Express **13**, 6296–6304 (2005).

#162342 - $15.00 USD Received 31 Jan 2012; revised 14 Mar 2012; accepted 14 Mar 2012; published 27 Apr 2012

9. F. Pfeiffer, O. Bunk, C. David, M. Bech, G. Le Duc, A. Bravin, and P. Cloetens, "High-resolution brain tumor visualization using three-dimensional x-ray phase contrast tomography." Phys. Med. Biol. **52**, 6923–6930 (2007).
10. G. Schulz, T. Weitkamp, I. Zanette, F. Pfeiffer, F. Beckmann, C. David, S. Rutishauser, E. Reznikova, and B. Müller, "High-resolution tomographic imaging of a human cerebellum: comparison of absorption and grating-based phase contrast." J. R. Soc. Interface **7**(53), 1665–1676 (2010).
11. T. Weitkamp, I. Zanette, C. David, J. Baruchel, M. Bech, P. Bernard, H. Deyhle, T. Donath, J. Kenntner, S. Lang, J. Mohr, B. Müller, F. Pfeiffer, E. Reznikova, S. Rutishauser, G. Schulz, A. Tapfer, and J.-P. Valade, "Recent developments in x-ray Talbot interferometry at ESRF-ID19," Proc. SPIE **7804**, 780406 (2010).
12. J. Herzen, T. Donath, F. Pfeiffer, O. Bunk, C. Padeste, F. Beckmann, A. Schreyer, and C. David, "Quantitative phase-contrast tomography of a liquid phantom using a conventional x-ray tube source," Opt. Express **17**, 10010–10018 (2009).
13. G.-H. Chen, J. Zambelli, K. Li, N. Bevins, and Z. Qi, "Scaling law for noise variance and spatial resolution in differential phase contrast computed tomography," Med. Phys. **38**, 584–588 (2011).
14. J. Zambelli, N. Bevins, Z. Qi, and G.-H. Chen, "Radiation dose efficiency comparison between differential phase contrast CT and conventional absorption CT," Med. Phys. **37**, 2473–2479 (2010).
15. K. J. Engel, D. Geller, T. Köhler, G. Martens, S. Schusser, G. Vogtmeier, and E. Rössl, "Contrast-to-noise in x-ray differential phase contrast imaging," Nucl. Instrum. Meth. A **648**, 202–207 (2010).
16. M. Bech, "X-ray imaging with a grating interferometer," Ph.D. thesis, University of Copenhagen (2009).
17. T. Thuering, P. Modregger, B. R. Pinzer, Z. Wang, and M. Stampanoni, "Non-linear regularized phase retrieval for unidirectional X-ray differential phase contrast radiography," Opt. Express **19**, 25545–25558 (2011).
18. J. Hsieh, *Computed Tomography - Principles, Design, Artifacts, and Recent Advances*, 2nd ed. (Wiley, Hoboken, NJ, 2009).
19. A. V. Oppenheim and R. W. Schafer, *Discrete-Time Signal Processing*, 2nd ed. (Prentice-Hall, Upper Saddle River, NJ, 1999).
20. R. C. Gonzalez and R. E. Woods, *Digital Image Processing*, 3rd ed., Vol. 3 of Texts in Computer Science (Pearson Prentice Hall, Upper Saddle River, NJ, 2008).

1. Introduction

Traditional X-ray imaging uses attenuation to produce image contrast. In recent decades however the possibility of using the refractive properties of a sample for imaging has been investigated, [1–3] leading to the field of X-ray phase-contrast imaging. It has been demonstrated on multiple occasions that X-ray phase-contrast is superior to attenuation contrast under certain conditions. This improved contrast originates from the small photo-electric absorption cross-section of low-Z materials in the $10 - 100$ keV range. [4] As a consequence, X-ray phase-contrast imaging appears especially promising for imaging soft tissue, where the traditional attenuation contrast is usually limited, unless contrast agents are used.

A quantification of the performance of phase contrast compared to attenuation contrast is difficult because of the differences in the image formation process. While an attenuation-contrast image can be interpreted as a simple projection of an object function (the distribution of linear absorption coefficient), the relation of phase-contrast images to the corresponding object function (the decrement of the X-ray refractive index) is usually not as simple. Among the many different methods for obtaining X-ray phase-contrast images that have been reported so far, one that seems particularly promising for clinical applications is grating-based imaging using a Talbot interferometer. [5–11] This approach produces differential phase contrast (DPC), i.e. it yields phase contrast in the form of the derivative of the total phase shift produced by a sample. The attenuation image can also be extracted from the data without additional acquisition effort. Due to the differential nature of the phase contrast signal a comparison to attenuation contrast is especially relevant. Area contrast, on the other hand, is predominantly visualized in the attenuation image, typically dominated by low spatial frequencies.

One way to directly compare both contrast signals is quantitative phase-contrast computed tomography (PC-CT), [12–14] where the differential phase-contrast images are inherently integrated by the reconstruction algorithm, resulting in an image proportional to the decrement of the refractive index. But for radiographic applications such as mammography, where the interest in increased soft tissue contrast and the requirement for low radiation dose is especially

#162342 - $15.00 USD Received 31 Jan 2012; revised 14 Mar 2012; accepted 14 Mar 2012; published 27 Apr 2012

high, usually only a single projection is recorded. This gives rise to the question of how to assess and compare image quality and information content in the domain of single projections or in other words, how to compare a non-differential to a differential signal.

In this paper we introduce a quantity, the "Relative Contrast Gain" (RCG), which provides an estimate of the expected performance of a differential phase-contrast image compared to an attenuation projection. It is defined as the ratio of the contrast-to-noise ratio (CNR) in a DPC projection to the CNR in an attenuation projection and it is meant as a analysis tool that can be applied on real data. Engel et al. [15] recently derived a theory of CNR in differential phase-contrast imaging based on an integration of the phase. In contrast to the approach of Engel et al., here we propose to solve the problem of comparing the two image modalities by differentiating the attenuation image along the same direction as the derivative of the phase.

2. The relative contrast gain

To motivate the use of a differential attenuation signal for the analysis of the RCG, we express the attenuation and the phase contrast in terms of the sample's space-dependent complex index of refraction,

$$n = 1 - \delta + i\beta. \tag{1}$$

The decrement of the real part of the refractive index, δ, leads to a refraction of the incident X-rays and the imaginary part of the refractive index, β, is responsible for attenuating incoming X-rays. From a single measurement we extract a 2D transmission map, which we call $I(x,y)$, and a 2D differential phase map $\alpha(x,y)$, which denotes the spatial distribution of the angular refraction of the X-rays after having passed the sample. From these measured quantities we derive the following physical quantities: [16]

$$T(x,y) = \ln\left(\frac{I(x,y)}{I_0(x,y)}\right), \tag{2}$$

$$\partial_x \Phi(x,y) = \frac{2\pi}{\lambda}\alpha(x,y), \tag{3}$$

where λ is the wavelength of the X-ray beam and $I_0(x,y)$ denotes the intensity of the incident beam at each position of the transmission map. We use ∂_x as a shorthand definition for the partial derivative along a direction x.

The relative transmission T is proportional to the projection of β along z, i.e. $\int \beta \, dz$ and the total phase shift Φ is proportional to $\int \delta \, dz$, where z is the beam propagation direction. Note that from a single projection we can only obtain these line integrals of the two quantities through the sample.

In any experiment, noisy versions of T and Φ are measured, and our task is to compare the quality of these two signals. To obtain a physically meaningful comparison we can either differentiate eq. (2) or integrate eq. (3). Integration of eq. (3) is difficult to accomplish due to the missing constant of integration and an extremely low signal-to-noise ratio of the non-zero low frequency components, which can lead to strong artifacts. [17] We now see from the equations that the only other possibility for comparison is to differentiate eq. (2) along the same direction x as the derivative in eq. (3). As a result we get the following definition for the differential transmission:

$$\partial_x T = \frac{\partial}{\partial x}\ln\left(\frac{I}{I_0}\right). \tag{4}$$

The main concept behind the definition of the Relative Contrast Gain is a quantification of the increase in feature contrast of differential phase contrast compared to attenuation projections.

#162342 - $15.00 USD Received 31 Jan 2012; revised 14 Mar 2012; accepted 14 Mar 2012; published 27 Apr 2012

For the analysis the following definition of a contrast-to-noise ratio (CNR) is used:

$$\mathrm{CNR} = \frac{\max(\mathrm{A}) - \min(\mathrm{A})}{\sigma_0}, \tag{5}$$

where A denotes a set of image values in a region of interest (ROI) in a projection and σ_0 is the standard deviation of image values in a flat region, i.e. the pure image noise. This definition can be seen as an effective dynamic range or in other words the number of grey levels needed to represent the image without loss of information. For a comparison of differential phase-contrast projections to attenuation projections we then define the RCG as the ratio of the CNR in a ROI of the differential phase projection to the CNR in the same ROI of the differential attenuation projection,

$$\mathrm{RCG} = \frac{\mathrm{CNR}_\Phi}{\mathrm{CNR}_T} = \frac{\Delta(\partial_x \Phi)/\sigma_{\partial_x \Phi}}{\Delta(\partial_x T)/\sigma_{\partial_x T}}, \tag{6}$$

where $\Delta(X)$ corresponds to $\max(X) - \min(X)$ and σ_X denotes the standard deviation.

The RCG is an estimate of the relative contrast of phase projections and attenuation projections. By normalizing on the standard deviation of the respective images, the pure image signals, that are not hidden by noise, are compared. In imaging terms we could also reformulate that by saying that the RCG is a quantity that determines which signal provides a larger dynamic range in the presence of noise. It is similar to the detective quantum efficienty (DQE), which quantifies the ability of an imaging system or detector to provide good signal-to-noise.

2.1. Differentiation of the attenuation image

The problem of differentiating a discrete image affected by noise presents a challenge that is difficult to solve. This is due to a low signal-to-noise ratio in high frequency components found in most images, where the derivative will lead to an amplification of the noise levels. It is well known that the derivative corresponds to a linear function in Fourier space. In analogy to the Ram-Lak filter known from the reconstruction in attenuation computed tomography [18, 19] we have to bandlimit the filter response by applying a window function. Typical choices in CT reconstructions are the Dirichlet-window (rectangle-window), *sinc*-window, Hamming-window or the Hann-window. [18, 19] As images are functions that are sampled on a finite grid and spatially limited, their Fourier transform will be inherently bandlimited with a cutoff frequency of $1/2$ pixel^{-1}. To prevent aliasing effects that may be introduced by applying a discrete Fourier transform, the filter also has to be bandlimited and, as in the case of CT reconstruction filters, there are certain degrees of freedom in choosing the shape of a bandlimiting window function. The two main concerns in choosing the appropriate window function are the accuracy of the resulting derivative and the best possible noise suppression without losing image information, i.e. spatial resolution.

For the present application of differentiating the attenuation image the Dirichlet-window was compared to the Hamming- and a Gaussian-window. We chose the Gaussian-derivative filter [20] because it is the most versatile one. In the following we will set the width $\sigma = 1/2\pi$ pixel^{-1}. This corresponds to a derivative filter combined with a smoothing operation over one pixel in image space. Smoothing in *y*-direction by the same amount improves the noise suppression even further. Smoothing by this small amount is just enough to keep the noise at an acceptable level. Using a smaller σ, i.e. smoothing over a larger area of pixels in image space, leads to a visual degradation of the image and a loss of information.

3. Results

To validate the concept, we have applied the RCG analysis on experimental data and we present first results in the following. For that purpose, radiographs of a human breast sample were

#162342 - $15.00 USD Received 31 Jan 2012; revised 14 Mar 2012; accepted 14 Mar 2012; published 27 Apr 2012

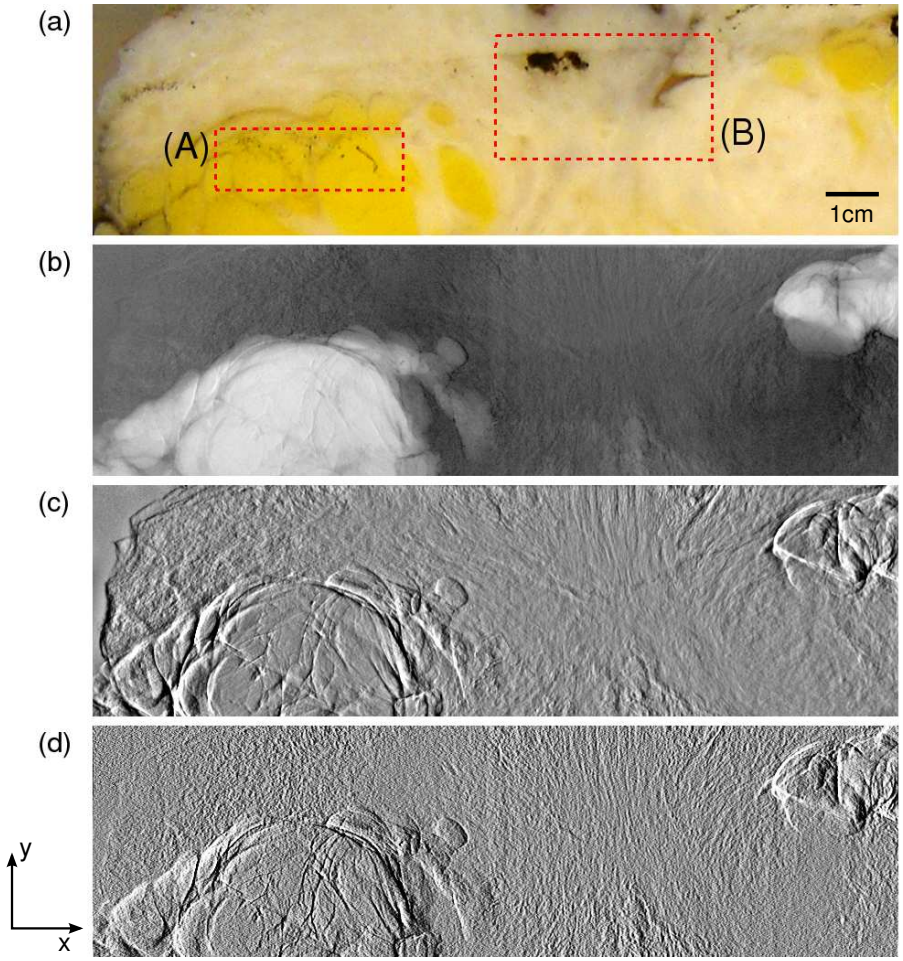

Fig. 1. overview of the experimental data used in the analysis. Panel (a) shows a photograph of the breast sample. The RCG method is applied on the two distinct sample regions marked (A) and (B) in the photograph. Panel (b) shows the transmission T for the same region as in the photograph. This projection is the attenuation signal and proportional to $\ln(I/I_0)$. In panel (c) the differential phase projection is shown. It is proportional to α and shows the signal according to eq. (3). Both projections are obtained from the same set of raw projections from a grating interferometer experiment. Finally, panel (d) shows the derivative of the attenuation signal, i.e. the projection proportional to $\partial_x T$. It represents the signal according to eq. (4). The projections in panels (b-d) have pixel dimensions of 1300x373.

#162342 - $15.00 USD Received 31 Jan 2012; revised 14 Mar 2012; accepted 14 Mar 2012; published 27 Apr 2012

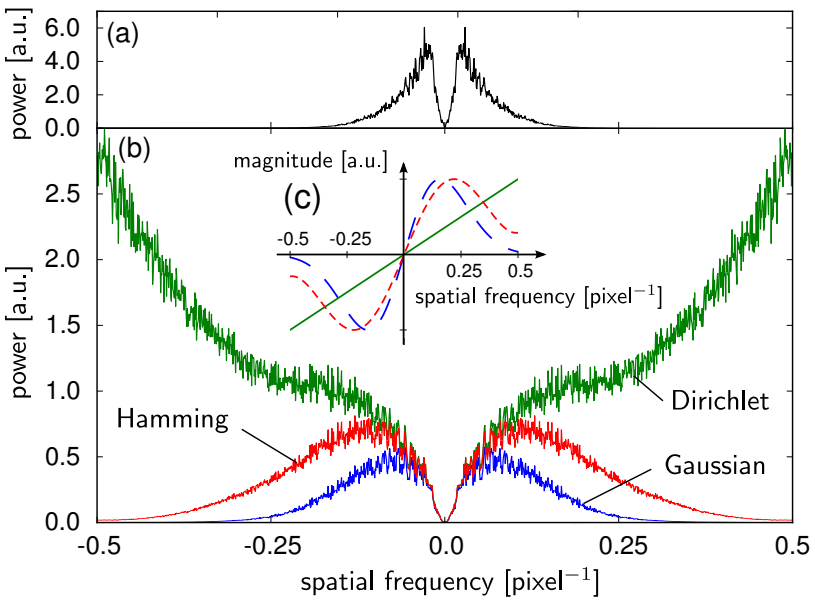

Fig. 2. power spectra of the experimental data shown in fig. 1, calculated by computing the absolute squared Fourier transform in *x*-direction for each image row and averaging in *y*-direction. (a) power spectrum of the DPC projection, (b) power spectra of the differential attenuation projection calculated with different filter functions as indicated in the figure, (c) corresponding filter functions (solid green: Dirichlet windowed, short-dashed red: Hamming windowed, long-dashed blue: Gaussian windowed with $\sigma = 1/2\pi$ pixel^{-1}).

recorded using a two-grating Talbot interferometer [8–11] at the ID19 beamline of the European Synchrotron Radiation Facility in Grenoble, France. The radiographs were taken with a monochromatic X-ray beam with an energy of 23 keV in the 9$^{\text{th}}$ fractional Talbot order. The distance between the phase grating G_1 and the analyzer grating G_2 was $d = 0.48$ m, G_1 had a period of $g_1 = 4.785\,\mu$m and G_2 a period of $g_2 = 2.4\,\mu$m. Phase stepping was performed in four steps over one period. The resulting raw images are processed with the established Fourier phase-stepping analysis [8] to extract the relative transmission signal T and the differential phase signal α. [16] The sample itself was a slice of human breast tissue about 1 cm thick, fixated in formalin. Figure 1 gives an overview of the experimental data used in the analysis.

For the RCG analysis the attenuation signal was brought into the form introduced in the first section, more specifically eq. (4), to be able to compare the two signals. More precisely, we took the logarithm of the attenuation signal and differentiated it using the Gaussian-derivative filter defined in the previous section. We used eq. (3) as it is, as the differential phase signal is directly available from the phase-stepping analysis. To ensure a fair comparison, a Gaussian filter with the same width was also applied to the DPC signal. This introduces the same loss of high frequency information that occurs during the differentiation of the attenuation signal. The noise standard deviation of both signals was calculated from corresponding reference projections, i.e. from a blank scan without the sample in the beam.

Figure 2 shows power spectra for the experimental data shown in fig. 1 to assess the behaviour of the different filter functions when applied to the attenuation projection and to compare them to the DPC projection. The power spectrum of the differential phase contrast projection is plotted in panel a). Panel b) shows the power spectra of the attenuation projection differentiated using the three indicated window functions. Finally in panel c) the filter functions themselves

#162342 - $15.00 USD Received 31 Jan 2012; revised 14 Mar 2012; accepted 14 Mar 2012; published 27 Apr 2012

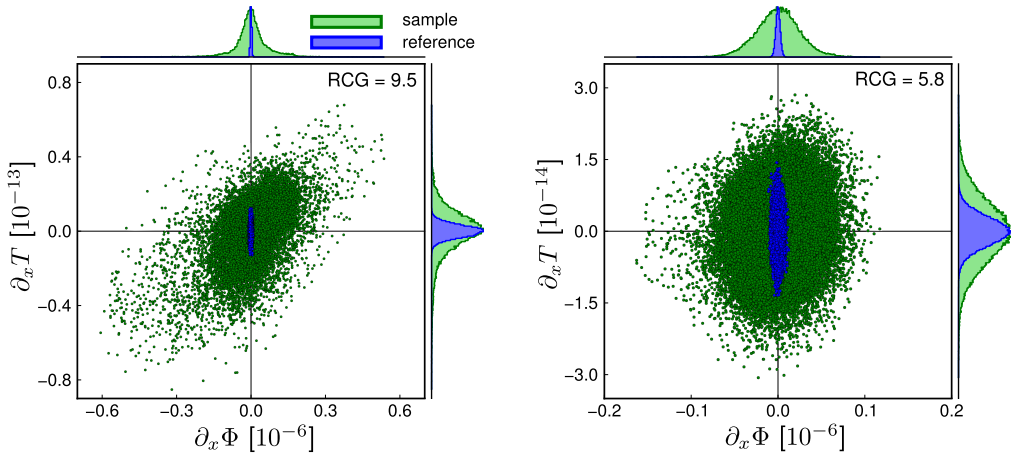

Fig. 3. In the main part of each subfigure the values of $\partial_x T$ and $\partial_x \Phi$ for each position (x,y) in the projection are presented in the form of a scatterplot for regions (A) (left) and (B) (right), respectively. The horizontal axis corresponds to the differential phase-contrast projection, the vertical axis to the differential attenuation projection. Histograms showing the distribution of values for both signals for the sample and reference (i.e. blank scan) regions are plotted on top of the respective axes of the signals. Green color denotes the sample region and blue the corresponding reference regions. The definition of the RCG in eq. (6) can equivalently be stated in terms of the geometry of the ellipses formed by the pixel values of the sample region and the widths of the reference region histograms. The width of the ellipse corresponds to $\Delta\partial_x\Phi$ and the height corresponds to $\Delta\partial_x T$. This means that the RCG is inversely proportional to the slope of the ellipses major axis.

are plotted. These plots show that the Gaussian-derivative filter with $\sigma = 1/2\pi$ pixel^{-1} performs reasonably well in making the power spectrum of the attenuation projection similar to that of the differential phase contrast projection.

A visual representation of the RCG is given in fig. 3 for regions (A) and (B) defined in fig. 1, respectively. Using eq. 6 we find for region (A) an $\mathrm{RCG_A} = 9.5$ and for region (B) an $\mathrm{RCG_B} = 5.8$.

4. Discussion and conclusion

The results of the RCG analysis from the last section indicate that phase-contrast projections, as expected, can provide substantially higher soft-tissue contrast than attenuation imaging. Two distinct regions of interest were analyzed, one with clearly visible features and one with features that are barely visible by the human observer. Looking at the scatterplots and histograms in fig. 3 and comparing the width and height of the ellipses formed by the sample (green) and reference (blue) pixel values and the widths of the corresponding projections in the 1-D histograms it is obvious that in both regions the fraction of the signals dynamic range covered by noise is larger for the differential attenuation. This observation is quantified by RCG values of 9.5 and 5.8 for regions (A) and (B) respectively, confirming the improved CNR performance of differential phase projections. The RCG is different for these two regions, which indicates that the RCG analysis depends strongly on the properties of the analyzed region. We believe that this is mainly due to the different spatial frequencies contained in these two regions and the different ratios of δ/β for different materials. Therefore the RCG is a local measure that states for which regions the phase signal should be trusted more than attenuation. Because of

#162342 - $15.00 USD Received 31 Jan 2012; revised 14 Mar 2012; accepted 14 Mar 2012; published 27 Apr 2012

the uncertainty in choosing the width of the Gaussian-derivative filter that is used to calculate $\partial_x T$, the RCG cannot be defined as an absolute scale, but rather a relative measure to compare different regions inside an image. Further work has to be done on calibrating the derivative filter to be able to absolutely quantify the contrast improvement of differential phase contrast compared to attenuation contrast, a task especially difficult because of the different noise power spectra in the attenuation and phase components.

The results we obtained for the RCG can, in principle, be further improved by optimizing the experimental setup. For the experimental data of the human breast tissue the visibility of the fringe oscillations during the phase-stepping was 54%. As the noise in a phase-contrast projection is inversely proportional to this visibility we can reach higher contrast-to-noise in the phase projection by increasing the visibility. Note that a change in visibility will not affect the CNR of the attenuation projection which will result in a higher relative contrast gain in favor of phase contrast. There are several ways to improve an experimental setup in terms of visibility. The manufacturing of phase and absorption gratings is constantly improving, leading to fewer defects in the gratings and to higher aspect ratios allowing X-rays with higher energies to be used. Also having the gratings matched to the desired X-ray energy and adjusting the Talbot distance between the phase grating and the absorption grating accordingly may improve the visibility.

Our results are consistent with those presented recently by Engel et al. [15] and we conclude that the RCG formalism can be used as a tool to assess the image quality in differential phase-contrast imaging. Also, the discussions in this paper and in Engel et al. [15] indicate that the details of an experimental setup, e.g. quality of the gratings, influence only the CNR of the phase projection but not the attenuation image, so from this fact we conclude that the RCG can be used as a tool to compare the performance of different experimental setups.

In summary we have presented the Relative Contrast Gain as a simple and practical tool to determine the relative contrast-to-noise-ratio of the attenuation- and differential phase-contrast signals that are available from grating-based X-ray imaging. The attenuation projection was differentiated to bring it into a comparable modality to the differential phase projection using a Gaussian-windowed derivative filter based on the Fourier derivative theorem. The Relative Contrast Gain was then defined as the ratio of the contrast-to-noise ratio of a region of interest in the differential phase projection to the contrast-to-noise ratio in the same region in the differential attenuation projection. We applied the RCG analysis on experimental data of human breast tissue aquired on a grating-based imaging setup, yielding an RCG of 9.5 for a region containing strong features and 5.8 for a region with barely visible features. This indicates that the RCG is a local measure depending on the properties of the analyzed material.

Acknowledgments

The authors acknowledge ESRF for granting beamtime (proposal MI-983) and the kind help of the ID19 beamline staff during the experiments. D.H., P.T., M.B., M.S., S.S., and F.P. acknowledge financial support through the DFG Cluster of Excellence Munich-Centre for Advanced Photonics and the European Research Council (FP7, Starting grant #240142). T.W. acknowledges support from DIGITEO-Triangle de la Physique (grants 2009-034T and 2009-79D). This work was carried out with the support of the Karlsruhe Nano Micro Facility (KNMF), a Helmholtz Research Infrastructure at Karlsruhe Institute of Technology (KIT).

#162342 - $15.00 USD Received 31 Jan 2012; revised 14 Mar 2012; accepted 14 Mar 2012; published 27 Apr 2012